HHS Public Access

Author manuscript

Arch Clin Exp Dermatol. Author manuscript; available in PMC 2023 June 12.

Published in final edited form as:

Arch Clin Exp Dermatol. 2021 April ; 3(1): . doi:10.46527/2583-6374.119.

Macrophage Response to Simulated Solar Radiation in the Development of Human Malignant Melanoma

Sherman Chu[1,2,*,†], **Tatyana A Petukhova**[3,†], **Jeremy S Bordeaux**[1], **Thomas S McCormick**[1], **Kevin D Cooper**[1]

[1]Department of Dermatology, University Hospitals Cleveland Medical Center, Cleveland, OH, USA

[2]Western University of Health Sciences, College of Osteopathic Medicine of the Pacific, Northwest, Lebanon, OR, USA

[3]Weill Cornell Medical College, New York, NY, USA

Abstract

Background: IFN-γ is widely debated regarding its purported anti- or pro-tumorigenic properties. We initiated a pilot study of primary malignant melanoma patients to investigate whether macrophage-derived IFN-γ is produced in humans as proposed in murine melanomagenesis models.

Methods: Biopsy specimens of fresh-frozen primary melanoma tissue were used to quantify co-localization of IFN-γ, macrophages, lymphocytes, and downstream IFN-γ signatures. Additionally, we analyzed simulated solar radiation (SSR) exposed skin in patients with a history of melanoma versus healthy controls to compare the relative magnitude of macrophage infiltration.

Results: Our data identified a subset of tumor infiltrating $CD68^+$ macrophages that co-localized with IFN-γ (Pearson's Correlation = 0.33 ± 0.11) in patients with primary melanoma (Stage 0-III). Additionally, a population of infiltrating $CD3^+$ lymphocytes strongly co-localized with IFN-γ (Pearson's Correlation = 0.57 ± 0.11). Malignant melanoma cells were double positive for downstream IFN-γ response elements, MIG/CXCL9, and phosphorylated STAT-1 (P-STAT-1). Cellular signaling pathways were also observed when we exposed the skin of melanoma patients to SSR. Despite robust CXCL9 expression in the epidermis of SSR-exposed skin of melanoma patients, we observed decreased macrophage infiltration into melanoma patient skin.

[*]**Corresponding author:** Chu S, Department of Dermatology, University Hospitals Cleveland Medical Center, 11100 Euclid Avenue, Cleveland, OH 44106, USA, Tel: +1 216-368-2000, sxc1407@case.edu.

[†]These authors contributed equally to this work.

Author contributions

S.C., T.S.M., and J.S.B. contributed to methodology. T.A.P., K.D.C., T.S.M., and J.S.B. contributed to data curation. T.A.P., T.S.M, and K.D.C. contributed to formal analysis. K.D.C., T.S.M., and J.S.B. contributed to funding acquisition. T.A.P. and T.S.M. contributed to investigation. K.D.C., T.S.M., and J.S.B. contributed to obtaining resources. K.D.C., T.S.M., and J.S.B. contributed to supervision of the project. S.C., T.S.M., K.D.C., and J.S.B. contributed to validation of data. T.A.P., K.D.C., T.S.M., and J.S.B. contributed to the writing of the original draft. S.C., K.D.C., T.S.M., and J.S.B. contributed to the review and editing of the article. All authors read and approved the final version of the manuscript.

Ethics Approval

Our study was approved by the University Hospitals Cleveland Medical Center Institutional Review Board (CC00152).

Conflict of Interest Disclosures

Authors declare no conflict of interests for this article.

Conclusion: Peritumoral macrophages in melanoma patient skin produce IFN-γ and melanocytes appear to exhibit in vivo responsiveness to IFN-γ, such as P-STAT-1 and upregulated CXCL9 expression. However, despite producing CXCL9 in response to SSR, the normal skin of melanoma patients demonstrates a weak leukocyte infiltration. Immune-modulatory studies for the prevention or treatment of human malignant melanoma may need to address complex tissue and melanocyte signaling and crosstalk.

Keywords

Interferon-gamma; Macrophage; Macrophage chemotactic factors; Melanoma; Ultraviolet radiation

1. Introduction

Skin cancer is the most common cancer in the United States and is the cause of over 60% of all skin-disease related deaths [1]. Melanoma accounts for 5.6% of new cancers in the U.S and is responsible for 1.1% of all cancer-related deaths in the country [2]. Additionally, incidence rates for melanoma have been steadily increasing over the past two decades [3].

Ongoing carcinogenesis research has resulted in an increased understanding of mutations that initiate the development of cutaneous melanoma. Ultraviolet radiation (UVR), including ultraviolet A (UVA), can generate reactive oxygen species capable of damaging proteins and DNA, and promoting carcinogenesis [4]. However, the exact pathogenetic factors and mechanisms that initiate this malignant transformation are not fully understood.

Melanocytes represent an incredibly small percentage of total skin cells (~1%), making it difficult to efficiently isolate. However, a mouse model has been created to investigate melanocyte transformation [5]. The model allowed melanocyte imaging and isolation following UV radiation, revealing that interferon-γ (IFN-γ)-secreting macrophages were recruited towards the epidermis following ultraviolet B (UVB) exposure, resulting in melanocytic cell survival and immune system evasion. Notably, the blockade of IFN-γ mediated by antibodies stopped macrophage promotion of melanoma growth and survival [5].

IFN-γ is widely debated for its anti-tumorigenic or pro-tumorigenic properties. Studies have found that IFN-γ can directly inhibit tumor growth and cause apoptosis of tumor cells [6,7], whereas contrasting studies have shown that IFN-γ promotes melanoma cell survival by various processes under certain circumstances by inhibiting apoptosis [5, 8]. Additionally, previous clinical trials have found no therapeutic efficacy of systemic IFN-γ in treating melanoma patients [9,10].

Furthermore, tumor-associated macrophages (TAMs), a class of immune cells described as M2 type-like macrophages, have been reported to inhibit anti-tumor immune responses and promote angiogenesis of tumor cells [11]. These TAMs contribute to the tumor microenvironment (TME) that suppresses the immune system. Tumor-infiltrating lymphocytes (TILs), a group of lymphocytes within the TME is a positive prognostic indicator in melanoma. In contrast, M2 macrophages have been found to inhibit $CD8^+$

cytotoxic T lymphocyte (CTL) activity, which may result in decreased survival in melanoma patients [12]. Macrophage infiltration has been demonstrated to correlate with worse survival in stage I/II disease and are more abundant in invasive melanomas, while infiltrating CTLs were found to be spatially closer to non-proliferating tumor cells [13,14]. The immunosuppressive processes of macrophages require close proximity or even direct contact with CTLs, stressing the importance of analyzing spatial relationships within the TME.

In order to effectively detect the activity of IFN-γ, we examined downstream targets of IFN-γ (MIG/CXCL9, P-STAT-1) that have been reported to exhibit a longer detectable half-life. In particular, MIG/CXCL9, a chemokine induced by IFN-γ produced by activated macrophages, is regarded as a marker for activated macrophages. MIG/CXCL9 and its receptor CXCR3 have been associated with melanoma development and solar simulated radiation (SSR)-induced skin inflammation [11,15,16]. Additional studies have shown that primary melanoma lesions have T-cell infiltrates that express higher levels of MIG/CXCL9 and may lead to migration of melanoma cells, resulting in suppression of T-cells and melanoma metastases [11,17,18].

In this study, we examined and quantified the co-localization of IFN-γ, macrophages, lymphocytes, and downstream IFN-γ signatures in human melanoma tissue samples using immunofluorescence confocal microscopy. Additionally, we examined SSR-exposed skin in patients with a history of melanoma and in healthy controls to compare and quantify the relative magnitude of macrophage infiltration.

2. Materials & Methods

2.1 Screening and study design

The Institutional Review Board at University Hospitals Cleveland Medical Center (UHCMC) approved this pilot observational study. Ten active malignant melanoma patients were screened, provided written informed consent, and enrolled into a pilot observational case-series clinical study. Patients with biopsy-proven melanoma that was not fully excised on biopsy were scheduled to have the residual malignant tissue re-excised with margins of healthy, benign skin to fulfill medical standard of care. Prior to treatment with wide local excision, punch biopsies were sampled from the remaining visible melanoma lesion and from an adjacent uninvolved site to serve as an internal control. Samples were snap-frozen in optimal cutting temperature (OCT) compound in liquid nitrogen and processed for immunofluorescence confocal microscopy. A dermatopathologist confirmed the presence of residual melanoma in hematoxylin and eosin stained slides of samples biopsied prior to microscopic analysis.

Another set of seven melanoma patients and four controls were screened for eligibility, provided written informed consent, and enrolled into a two-arm, case-control, observational pilot study to analyze patient response to SSR. Each of the five patients who completed the study had a history of invasive melanoma and four (80%) were observed to have a recurrence of their melanoma. Subjects were exposed to 3 times the minimal erythema dose (MED) of SSR on a non-sun exposed area (i.e., buttocks, medial thighs, medial arms) using a solar simulator lamp that closely resembles the spectrum of natural sunlight (9% UVA and

91% UVB), as previously performed [19]. After 32 hrs, punch biopsies completely excised the irradiated skin in order to confer no additional risk to patients concerning SSR exposure. A biopsy of adjacent non-irradiated skin was also collected to serve as an internal control. Biopsy specimens were snap-frozen in OCT compound and processed into frozen sections (5 μm −10 μm) for immunofluorescent microscopic analysis.

2.2 Immunofluorescence confocal microscopy

Biopsy samples were embedded into OCT compound and frozen at −80ºC until fixation and immunohistochemistry analysis. Cryosections (7 μm) were cut onto ProbeOn-Plus (Fisher Scientific) glass slides from frozen OCT embedded tissue blocks. Slides and samples were air-dried, fixed in acetone at −20ºC for 10 min, rehydrated in phosphate-buffered saline (PBS), and blocked with 10% goat serum for 30 min. Blocked sections were incubated in primary antibodies diluted in 10% goat serum/PBS overnight at 4ºC or for 3 hrs at room temperature. Sections were washed in large volumes of PBS three times for 5 min and co-stained with isotype-specific goat secondary antibodies conjugated to Alexa Fluor dyes (Invitrogen) for fluorescent detection. Alternatively, to minimize background signal and amplify the fluorescent signal, secondary antibodies directly conjugated to biotin were used and detected with streptavidin conjugated fluorophores, or horseradish peroxidase conjugated secondary antibodies and detected with tyramide conjugated fluorophores. If the sections were to be furthered incubated for triple-labeled immunofluorescence experiments, the sections were blocked with 10% mouse serum and primary antibodies directly conjugated to fluorophores were used sequentially after either overnight at 4ºC or for 3 hrs at room temperature. After washing with PBS, the slides were mounted in Vectashield (Vector Labs) self-hardening mounting media containing 4’,6-diamidino-2-phenylindole (DAPI) for nuclear detection.

All images were acquired using the UltraVIEW *VoX*™ spinning disk confocal system (PerkinElmer, Waltham, MA, USA) mounted on a Leica DMI6000B microscope (Leica Microsystems, Inc., Bannockburn, IL, USA) and equipped with a HCX PL APO 63x/1.4 objective. Confocal images of fluorescent markers of Alexa 647, Alexa 568, Alexa 488, and DAPI were collected using solid state diode lasers, with 640-nm, 488-nm, 561-nm and 405-nm excitation light, respectively, and appropriate emission filters. All confocal images were analyzed for co-localization using Volocity™ (PerkinElmer, Waltham, MA, USA) and MetaMorph™ Premier software (Molecular Devices Corporation, Sunnyvale, CA).

Primary mouse antibodies of differing isotypes targeting selected human antigens were chosen to not cross react in double- and triple-labeled immunofluorescence experiments. To serve as negative controls, all experiments were simultaneously duplicated with matching isotype control antibodies. Biopsies of psoriasis plaques served as positive control tissue for an intense inflammatory human skin microenvironment when testing new antibodies specific for immune cells of interest.

2.3 Statistical analysis

Descriptive statistics were used to summarize the distribution of tumor associated macrophages (CD68), lymphocytes (CD3), and IFN-γ producing cell types in human

melanoma tissue samples. Samples were analyzed according to delineated compartments defined as melanoma foci (area with tumor cell nests), interstitial space between foci (connective tissue separating solid tumor nests), and normal tissue. The adjacent control biopsies of healthy tissue were imaged according to structural compartments of epidermis, dermal-epidermal junction (DEJ), and the dermis. Co-localization was reported as the average and standard deviation of linear Pearson's correlations of the scatter plot between two channels in at least five high power fields per sample.

To examine and quantify the relative magnitude of macrophage infiltration following SSR exposure, descriptive statistics were used to summarize the outcome variables. The data for the two patient populations (melanoma patients and healthy controls) was analyzed to compare the SSR-exposed samples adjusted to the respective internal controls. Density of macrophage infiltration was reported as counts/mm epidermis in at least five power fields and reported as an average with standard deviation. Non-parametric analysis with Wilcoxon rank-sum test was used to investigate the association between density of macrophage infiltration and disease state.

3. Results

3.1 Discarded skin tissue

Ten volunteers with partially biopsied primary melanoma lesions were recruited for our study, nine of whom had residual melanoma confirmed by a clinical dermatopathologist (TABLE 1). Triple immunofluorescence was used for images of surface markers identifying macrophages (CD68), lymphocytes (CD3), and IFN-γ in melanoma tissue (FIG. S1). A subset of macrophages and lymphocytes were found to be co-localized with IFN-γ. Following the study, 3/10 (30%) of the patients had a recurrence of melanoma.

The majority of evaluated melanoma samples showed $CD68^+$ macrophages that infiltrate close to the primary tumor and penetrate the tumor nests. In contrast, dense lymphocytic beds were observed at a distance further from the primary tumor with a few scattered and activated IFN-γ producing lymphocytes infiltrating within the tumor nests. The predominant IFN-γ signal closest in proximity to MART-1 positive melanoma cells were associated with $CD68^+$ but not $CD3^+$ T cells (FIG. 1).

Quantitative analysis was performed on five random high-powered fields for each melanoma sample to calculate an average Pearson's Correlation of co-localization. The highest correlation was found between $CD3^+$ lymphocytes and IFN-γ (Pearson's Correlation = 0.57 ± 0.11, n=9). $CD68^+$ and IFN-γ demonstrated a lower correlation value (Pearson's Correlation = 0.31 ± 0.11; n=9) and no relative correlation between $CD3^+$ lymphocytes and $CD68^+$ macrophages was found (Pearson's Correlation = 0.11 ± 0.07, n=9) (FIG. S2, S3). This co-localization pattern was consistently observed for nine analyzed melanoma tumors, consisting of early and invasive superficial spreading and lentigo maligna melanoma subtypes.

Melanoma tissue identified with positive IFN-γ signaling were further analyzed for the presence of IFN-γ response signals. The presence and distribution of MIG/CXCL9, a

monokine induced by IFN-γ, was investigated to determine what cell types are responsive to the IFN-γ signaling cascade. Psoriasis tissue, known to be high in MIG/CXCL9, was used as a positive control (FIG. 2a). Melanoma tissue exhibited MIG/CXCL9 signals that were predominately limited to the melanocytic tumor nests with minimal co-localization of $CD68^+$ macrophages and no detectable co-localization with $CD3^+$ lymphocytes (FIG. 2b).

The detection of phosphorylated signal transducer and activator of transcription (STAT-1) was used as an additional marker for IFN-γ signal transduction. In response to IFN-γ, STAT-1 becomes phosphorylated on tyrosine and serine residues, resulting in dimerization and further activation of targeted gene expression. Tyrosine-phosphorylated STAT-1 (P-STAT-1) was expressed in several cell types in melanoma tissue, including $CD68^+$ macrophages, but was most highly co-localized to the melanoma tumor itself. We found that melanoma cells express an IFN-γ response signature (FIG. 2c, 2d).

Immunofluorescence for CXCR3, a MIG/CXCL9 cognate receptor, was performed to confirm the presence of the receptor on melanoma tissue (FIG. 2e, 2f). CXCR3 was highly expressed in melanoma cells, as well as in other cells present in the interstitial space between tumor nests (FIG. 2f).

3.2 Elicitation of CXCL9 in the epidermis of non-sun-exposed skin of melanoma patients exposed to simulated solar radiation

We hypothesized that aberrant CXCL9 expression, as a potential surrogate for IFN-γ signaling in melanoma, may already be a feature of non-sun-exposed skin in patients predisposed to acquiring melanoma. We examined CXCL9 expression in seven volunteers with a history of melanoma to determine whether differential skin responses are elicited by simulated solar radiation of non-sun-exposed skin as compared to controls. Five patients completed the study and four healthy volunteers were enrolled and serve as controls (TABLE 2). Skin samples were collected from patients with and without a history of melanoma 32 hrs after irradiation with three times the minimal erythema dose (3MED) of SSR to non-sun-exposed skin. An internal control of adjacent non-irradiated skin was also collected from each volunteer.

Using validated antibodies targeting macrophage surface markers, $CD68^+$ cells were counted in a delineated compartment of the papillary dermis. Cells were counted as macrophages if the fluorescent signal was double-labeled by two different antibodies and either adjacent to, or surrounded by, a nuclear DAPI signal. The counts were reported as densities per linear millimeter of epidermis. In melanoma patients, the average density of infiltrating macrophages was 61.8 counts/mm in irradiated skin and 51.9 counts/mm in non-irradiated skin, resulting in an average fold increase in dermal infiltrating macrophages of 1.19 ± 0.06. In healthy control subjects, the density of infiltrating macrophages was 67.7 counts/mm in irradiated skin and 48.8 counts/mm in non-irradiated skin, resulting in an average fold increase in dermal infiltrating macrophages of 1.37 ± 0.11 (FIG. 3). Melanoma patients exhibited a significantly decreased level of dermal infiltrating $CD68^+$ macrophages after UVB exposure compared to healthy controls (p=0.04).

A biopsy of UVB-exposed skin was taken 32 hrs post-irradiation to correspond with peak dermal macrophage infiltration [20]. Samples were additionally analyzed for downstream IFN-γ signaling for MIG/CXCL9 using immunofluorescence. All samples showed MIG/CXCL9 staining in the epidermis, which corresponds to keratinocyte labeling, as well as discrete staining of cells in the dermis, some being $CD68^+$ macrophages. Neither melanoma patients nor healthy controls exhibited a change in the intensity or location of the fluorescent signal following SSR (FIG. 4a–d). Melanoma tumor biopsies were found to exhibit a strong MIG/CXCL9 co-localized signal with malignant melanoma cells, leading us to co-stain SSR-exposed samples with Mart-1. Both healthy controls and melanoma patients did not exhibit co-localization of MIG/CXCL9 and Mart-1 positive melanocytes before and after SSR (FIG. 4e–h).

4. Discussion

Cutaneous melanoma is the most lethal of human skin cancers in the United States, and its incidence in young adults as well as in persons over the age of 50 has been steadily increasing over the last 30 years [21]. A large body of evidence supports the role of solar ultra-violet radiation (UVR), particularly intermittent high-intensity exposure, as a major environmental factor in the increased prevalence of this disease [22,23]. However, despite increased education and knowledge about the dangers of UVR, the lifetime risk of developing invasive melanoma continues to rise [24].

Zaidi *et al.* have proposed that IFN-γ secreting macrophages may be a potential link between UVB radiation and melanoma [5]. Using a murine model of melanomagenesis, they demonstrated that melanocytes exhibited increased activation, reduced apoptosis, and an IFN-γ response signature six days after acute inflammation induced by UVB exposure in the neonatal time period. In support of IFN-γ signaling facilitating melanoma progression in human subjects, Zaidi *et al.* demonstrated IFN-γ-secreting macrophages in samples of primary and metastatic human melanoma. Our data confirms the observation that macrophages are IFN-γ producers, as all tumors (100% of samples examined) contained extensive macrophage infiltration and exhibited a strong IFN-γ signature. Interestingly, the IFN-γ signal co-localized with a subset of $CD68^+$ macrophages, implicating differentiated macrophages in melanoma tissue as IFN-γ producers. In contrast to the data reported by Zaidi *et al.*, our melanoma samples also contained a large proportion of $CD3^+$ lymphocytes that were also strongly positive for IFN-γ. In all samples examined, we also observed that some cells were positive for only IFN-γ and neither $CD3^+$ nor $CD68^+$, suggesting another cell type may produce IFN-γ as well, potentially NK cells or $CD163^+$ tumor associated macrophages (TAMs) as suggested previously [25].

The current data demonstrate that the majority of IFN-γ positive cells are closely aligned with the tumor and some cells appear to invade the melanoma tumor nests. The data demonstrate that macrophages infiltrate in closer proximity to the tumor and even within the tumor nests, whereas lymphocytes are densely aggregated at a distance from the infiltrating macrophages.

The presence of immune cells in a tumor does not guarantee that an effective anti-tumor immune response will develop [26]. Studies have investigated leukocyte distribution in primary melanoma tumors, concluding that Breslow's depth and high melanoma cell proliferation are associated with higher rates of intra-tumoral $CD4^+$ and $CD8^+$ lymphocytes [27]. Consistent with the current study, authors also demonstrated that the majority of $CD3^+$ T cells reside in the peri-tumoral area [28]. Moreover, it has been demonstrated that a high amount of $CD3^+$ leukocytes predicts decreased survival, suggesting that although lymphocytes are able to target and infiltrate the tumor microenvironment, they may be unable to mount an effective immune response [29]. Several melanoma immune escape mechanisms have been proposed, including the secretion of immunosuppressive cytokines by the tumor itself and the defective or incomplete activation of killer T cells [30]. Additional studies of lymphocyte distribution in melanoma tumors have suggested that while $CD45^+$ cells may be consistently found infiltrating the tumor stroma, not all tumors contain detectable levels of IFN-γ signaling due to T cell suppression [31]. Our results suggest that the majority of T cells in the tumor microenvironment are activated as demonstrated by IFN-γ production and co-localization; however, the majority of these T cells are not in close proximity to the tumor and may be functionally incapable of inducing targeted melanoma cell death. Furthermore, as suggested by Zaidi *et al.* high levels of IFN-γ may promote a pro-tumorigenic response in melanocytes within the tumor [5].

The distribution of melanoma-specific macrophages has been previously investigated [14]. Macrophages are one of the predominant infiltrating cell types in melanomas and possess the dual ability to differentiate into either destructive anti-tumor M1 (classical) macrophages or pro-tumorigenic M2 cells (alternative) [32]. Macrophages, commonly referred to as tumor associated macrophages (TAMs) can suppress immune reactions, promote malignant proliferation, and enhance tumor vascularization [33]. Multiple studies have demonstrated that the presence of melanoma-specific TAMs correlates with a poor clinical prognosis [34–37]. Jensen *et al.* demonstrated that $CD68^+$ macrophages infiltrate melanoma tumor stroma, the tumor nests, and the melanoma invasive front, concluding that the presence of $CD68^+$ macrophage infiltration at the tumor invasive front is a predictor of poor survival, independent of ulceration and thickness, in patients with stage I-II melanoma [38]. Additional studies have shown that macrophage infiltration at the invasive front correlated with poor survival in early-stage melanoma, while the higher density of $CD8^+$, $CD3^+$, $CD45^+$, T cells, and B cells correlated with increased survival in metastatic melanoma [39,40]. Furthermore, a high CTL ratio and low macrophage density in the stroma and tumor has been reported to correlate positively with disease-specific survival and favorable prognosis in primary melanoma [12]. In this study, $CD68^+$ macrophage infiltration was a consistent feature of all melanoma samples with the additional finding of a subset of IFN-γ colocalization in macrophages within tumor nests, the invasive front, and in the tumor stroma. Further identification of downstream IFN-γ signaling elements was also demonstrated. Using a murine model of melanomagenesis, it has been demonstrated that upon UVB-induced DNA damage, IFN-γ-producing macrophages infiltrate the tissue and induce an IFN-γ response signature (increased mRNA levels of Ccl8, Ctla4, H2-K1 and H2-T23, etc…) in melanocytes that promotes immuneevasion of transformed cells [5,41]. In a study of human melanoma lymph node metastases, stimulation with IFN-γ induced

increased production of MIG/CXCL9, IP-10/CXCL10, and I-TAC/CXCL11 in melanoma cells (identified as $S100^+$ $CD45^{neg}$ $CD11c^{neg}$) and was confirmed by our data (FIG. 2). Interestingly, in the $CD45^+$ population, which includes $CD14^+$ cells, there was no significant staining for CXCL9–11. Upon examination of seven established melanoma cell lines, IFN-γ induced the production of CXCR3-cognate chemokines was observed in all of these cell lines [42].

Consistent with previous studies, we demonstrated that melanoma tumor cells were significantly co-localized with MIG/CXCL9 in primary melanoma tumors. These results confirm that unlike a chronic inflammatory tissue such as psoriasis, where $CD11b^+$ myeloid cells and keratinocytes were the major source of MIG/CXCL9 co-localization, melanoma cells induced by IFN-γ produce MIG/CXCL9 as the source of this signal, although we cannot determine from the current studies whether the primary source of IFN-γ signaling is lymphocyte or macrophage derived. We also demonstrated that melanoma cells were co-localized with P-STAT-1, suggesting long term activation to IFN-γ signaling and probable high levels of proliferation. The current study additionally confirms that primary melanoma cells themselves are able to respond to chemotactic MIG/CXCL9 signaling with the strong co-localization of the cognate receptor CXCR3 within melanoma cells.

Cause and effect relationships between SSR, IFN-γ signaling, and melanoma development was difficult to establish in the current experiments. We demonstrated that SSR-induced inflammation was associated with fewer infiltrating macrophages in melanoma patient tissue compared to healthy control volunteers; however, IFN-γ was not detected in resident macrophages prior to SSR irradiation, nor in SSR-induced macrophages in neither melanoma patients nor healthy controls. Several previous mRNA and immuno-histochemical studies of human skin have demonstrated that although IFN-γ is detectable in psoriatic plaques, healthy human skin does not exhibit detectable levels [43,44]. A more recent study of healthy human skin exposed to UVR has demonstrated that prior to UV irradiation at 4MED, an IFN-γ signal may be detected in up to 2% of resident perivascular $CD4^+$ lymphocytes. However, the author's demonstrated that IFN-γ mRNA was reduced to undetectable levels in the skin samples at 2 days and at 14 days post UVR exposure [45].

It is possible that our selected time course of maximal macrophage migration into the dermal tissues at 32 hrs is not an appropriate timeframe for transient IFN-γ induction that might have occurred as a burst earlier in the inflammatory process. In order to evaluate if IFN-γ signaling occurred prior to biopsy, the SSR biopsy samples were stained with downstream IFN-γ response elements such as MIG/CXCL9. The CXC chemokines are IFN-γ–induced small secretory proteins that are synthesized and released by leukocytes but have also been shown to be produced by epithelial, endothelial, and stromal cells [46]. Our data revealed basal levels of MIG/CXCL9 expression in keratinocytes and a subset of $CD68^+$ macrophages in all analyzed samples. MIG/CXCL9 expression was unaffected by UV irradiation in both melanoma patients and healthy controls. A similar pattern of MIG/CXCL9 expression in dermal infiltrating cells and basal keratinocytes has been reported in other dermal inflammatory conditions such as psoriasis and discoid lupus erythematosus [47]. Previous *in vitro* studies of cultured human keratinocytes with melanocytes exhibited a peak increase of MIG/CXCL production at 6 hrs post UVB irradiation. Thus, while

UVR-induced chemokine signaling may be elicited in the dermis, the current study is limited in detecting the MIG/CXCL9 change due to the biopsy collection point of 32 hrs after irradiation [15]. Additionally, the inflammatory changes occurring in the skin, may be more closely related to UVR itself and not necessarily connected to a downstream IFN-γ response. Additional analysis of IP-10/CXCL10, I-TAC/CXCL11, and P-STAT-1 may elucidate if other downstream IFN-γ signals exhibit a differential response in the skin after SSR exposure and those experiments are planned for future analysis.

Markers of apoptosis were also examined and did not reveal any melanocytes undergoing apoptosis in neither melanoma patients nor controls after SSR. Thus, our data is supportive of a proliferative signal. However, since the total number of melanocytes in the samples are small, the data is not conclusive in support of any anti-apoptotic effect.

Immune checkpoint inhibitors, namely anti-PD-1 therapy, has changed the treatment of melanoma. PD-1 and its ligand, PD-L1, are immune checkpoint molecules that suppresses T-cell activation and function. PD-L1 antibody therapy increases T-cell infiltration and IFN-γ production, resulting in the reduction of tumor growth [48,49]. Previous studies have shown that human TAMs express PD-1 and PD-L1 and that although the presence of TAMs correlates with a poor prognosis in cancer, macrophages can be induced to phagocytose tumor cells through SIRPα/CD47 blockade [50–52]. The blockade of PD-1 and PD-L1 *in vivo* increases TAM tumor cell phagocytosis, decreasing the tumor burden and growth in mice, suggesting that PD1 expression inhibits many cells in the TME, such as T-cells, B-cells, dendritic cells, and macrophages [51]. Mouse and human macrophages treated with PD-L1 antibodies have shown to be more abundant and larger than untreated macrophages and induces macrophage activation by upregulation of costimulatory molecules CD86 and MHC II, resulting in macrophage-mediated anti-tumor activity [53]. Furthermore, anti-PD-L1 was shown to remodel macrophages from a suppressive phenotype into a proinflammatory, immunostimulatory one, driven mainly by IFN-γ [54]. Our findings suggest that macrophage infiltration plays an important role in the development of melanoma, supporting the proposed mechanism of PD-1/PD-L1 blockade to macrophage activation and function.

An important limitation of the study was our small sample size. In the discard tissue portion of the study, it is difficult to draw conclusions about the results due to only having ten samples. Additionally, only superficial spreading and lentigo maligna melanoma subtypes were collected with no representation of acral, nodular, or mucosal melanomas and 50% of samples were early *in situ* melanomas. For the SSR exposure portion, recruitment of melanoma patients was the greatest limiting factor, resulting in the small sample size. Many melanoma patients are hesitant to purposely expose their skin to UVR, despite the relative safety of the procedure. There was an obvious bias towards melanoma patients that were not currently employed as the study required three separate visits to be completed on three consecutive days; most of the melanoma volunteers are retired males above the age of 60. Differences noted in the results of the SSR portion between the cases and controls may also be attributed to imperfect matching explained by the difficulty in age-matching healthy controls to melanoma patients.

An additional limitation to patient accrual is the time limit required for the three separate visits to be completed on three consecutive days. Most of the volunteers have been retired males above the age of 60. Similarly, it has been difficult to age-match healthy controls, as most of those volunteers are recruited from the student and work force population in the CWRU community. The differences noted in the results of the SSR study between the cases and controls may be attributed to imperfect matching and small sample size.

5. Conclusions

Our findings indicate that in melanoma tumors, IFN-γ-secreting macrophages infiltrate the tumor microenvironment and localize in the tissue. Additionaly, increased numbers of IFN-γ-secreting T cells are also observed in the peritumoral area. The high levels of IFN-γ-signaling appear to exert a downstream effect on melanoma cells, as evidenced by MIG/CXCL9 and P-STAT-1 co-localization. The melanoma cells themselves concomitantly display the CXCR3 cognate receptor and are able to respond to MIG/CXCL9 signaling in autocrine and paracrine fashions. These results confirm an active role of IFN-γ signaling in primary melanoma tumors, but the functional significance of pro- versus anti-tumorigenic role must be further elucidated in future work. The incidental finding of increased CXCR3 expression in keratinocytes in response to SSR suggests that the process may be independent of the IFN-γ-signaling cascade when direct DNA damage occurs. Additional studies of CXCR3 expression and SSR-related melanomagenesis may be a relevant approach for future experimentation.

Supplementary Material

Refer to Web version on PubMed Central for supplementary material.

6. Acknowledgement

Funding

Research reported in this publication was supported by the National Institute of Arthritis and Musculoskeletal and Skin Diseases of the National Institutes of Health under Award Numbers T32AR007569 and P30AR075048(SDRC). The content is solely the responsibility of the authors and does not necessarily represent the official views of the National Institutes of Health. This study was supported through funding from the Murdough Family Center for Psoriasis and Skin Diseases Research Center.

REFERENCES

1. Lim HW, Collins SAB, Resneck JS Jr., et al. The burden of skin disease in the United States. J Am Acad Dermatol. 2017;76(5):958–72 e2. [PubMed: 28259441]
2. National Cancer Institute. SEER Stats Fact Sheets: Melanoma of the skin: National Cancer Institute; 2020 [Available from: https://seer.cancer.gov/statfacts/html/melan.html.
3. Glazer AM, Winkelmann RR, Farberg AS, et al. Analysis of Trends in US Melanoma Incidence and Mortality. JAMA Dermatol. 2017;153(2):225–6. [PubMed: 28002545]
4. Khan AQ, Travers JB, Kemp MG. Roles of UVA radiation and DNA damage responses in melanoma pathogenesis. Environ Mol Mutagen. 2018;59(5):438–60. [PubMed: 29466611]
5. Zaidi MR, Davis S, Noonan FP, et al. Interferon-gamma links ultraviolet radiation to melanomagenesis in mice. Nature. 2011;469(7331):548–53. [PubMed: 21248750]
6. Chin YE, Kitagawa M, Kuida K, et al. Activation of the STAT signaling pathway can cause expression of caspase 1 and apoptosis. Mol Cell Biol. 1997;17(9):5328–37. [PubMed: 9271410]

7. Ikeda H, Old LJ, Schreiber RD. The roles of IFN gamma in protection against tumor development and cancer immunoediting. Cytokine Growth Factor Rev. 2002;13(2):95–109. [PubMed: 11900986]
8. Tanese K, Hashimoto Y, Berkova Z, et al. Cell Surface CD74-MIF Interactions Drive Melanoma Survival in Response to Interferon-gamma. J Invest Dermatol. 2015;135(11):2901.
9. Creagan ET, Ahmann DL, Long HJ, et al. Phase II study of recombinant interferon-gamma in patients with disseminated malignant melanoma. Cancer Treat Rep. 1987;71(9):843–4. [PubMed: 3113730]
10. Meyskens FL Jr., Kopecky KJ, Taylor CW, et al. Randomized trial of adjuvant human interferon gamma versus observation in high-risk cutaneous melanoma: a Southwest Oncology Group study. J Natl Cancer Inst. 1995;87(22):1710–3. [PubMed: 7473820]
11. Xiao P, Guo Y, Zhang H, et al. Myeloid-restricted ablation of Shp2 restrains melanoma growth by amplifying the reciprocal promotion of CXCL9 and IFN-gamma production in tumor microenvironment. Oncogene. 2018;37(37):5088–100. [PubMed: 29795405]
12. Gartrell RD, Marks DK, Hart TD, et al. Quantitative Analysis of Immune Infiltrates in Primary Melanoma. Cancer Immunol Res. 2018;6(4):481–93. [PubMed: 29467127]
13. Garcia-Martinez E, Gil GL, Benito AC, et al. Tumor-infiltrating immune cell profiles and their change after neoadjuvant chemotherapy predict response and prognosis of breast cancer. Breast Cancer Res. 2014;16(6):488. [PubMed: 25432519]
14. Salmi S, Siiskonen H, Sironen R, et al. The number and localization of CD68+ and CD163+ macrophages in different stages of cutaneous melanoma. Melanoma Res. 2019;29(3):237–47. [PubMed: 30399061]
15. Kurata R, Fujita F, Oonishi K, et al. Inhibition of the CXCR3-mediated pathway suppresses ultraviolet B-induced pigmentation and erythema in skin. Br J Dermatol. 2010;163(3):593–602. [PubMed: 20491766]
16. Robledo MM, Bartolome RA, Longo N, et al. Expression of functional chemokine receptors CXCR3 and CXCR4 on human melanoma cells. J Biol Chem. 2001;276(48):45098–105. [PubMed: 11571298]
17. Harlin H, Meng Y, Peterson AC, et al. Chemokine expression in melanoma metastases associated with CD8+ T-cell recruitment. Cancer Res. 2009;69(7):3077–85. [PubMed: 19293190]
18. Amatschek S, Lucas R, Eger A, et al. CXCL9 induces chemotaxis, chemorepulsion and endothelial barrier disruption through CXCR3-mediated activation of melanoma cells. Br J Cancer. 2011;104(3):469–79. [PubMed: 21179030]
19. Camouse MM, Domingo DS, Swain FR, et al. Topical application of green and white tea extracts provides protection from solar-simulated ultraviolet light in human skin. Exp Dermatol. 2009;18(6):522–6. [PubMed: 19492999]
20. Yoshida Y, Kang K, Berger M, et al. Monocyte induction of IL-10 and down-regulation of IL-12 by iC3b deposited in ultraviolet-exposed human skin. J Immunol. 1998;161(11):5873–9. [PubMed: 9834066]
21. American Cancer Society. Cancer Facts & Figures 2020. Atlanta ACS. 2020:1–60.
22. Trucco LD, Mundra PA, Hogan K, et al. Ultraviolet radiation-induced DNA damage is prognostic for outcome in melanoma. Nat Med. 2019;25(2):221–4. [PubMed: 30510256]
23. Rigel DS. Epidemiology of melanoma. Semin Cutan Med Surg. 2010;29(4):204–9. [PubMed: 21277533]
24. Garibyan L, Fisher DE. How sunlight causes melanoma. Curr Oncol Rep. 2010;12(5):319–26. [PubMed: 20623386]
25. Pettersen JS, Fuentes-Duculan J, Suarez-Farinas M, et al. Tumor-associated macrophages in the cutaneous SCC microenvironment are heterogeneously activated. J Invest Dermatol. 2011;131(6):1322–30. [PubMed: 21307877]
26. Allavena P, Sica A, Solinas G, et al. The inflammatory micro-environment in tumor progression: the role of tumorassociated macrophages. Crit Rev Oncol Hematol. 2008;66(1):1–9. [PubMed: 17913510]
27. van Houdt IS, Sluijter BJ, Moesbergen LM, et al. Favorable outcome in clinically stage II melanoma patients is associated with the presence of activated tumor infiltrating T-lymphocytes

and preserved MHC class I antigen expression. Int J Cancer. 2008;123(3):609–15. [PubMed: 18498132]

28. Hillen F, Baeten CI, van de Winkel A, et al. Leukocyte infiltration and tumor cell plasticity are parameters of aggressiveness in primary cutaneous melanoma. Cancer Immunol Immunother. 2008;57(1):97–106. [PubMed: 17602225]
29. Gooden MJ, de Bock GH, Leffers N, et al. The prognostic influence of tumour-infiltrating lymphocytes in cancer: a systematic review with meta-analysis. Br J Cancer. 2011;105(1):93–103. [PubMed: 21629244]
30. Mahmoud F, Shields B, Makhoul I, et al. Immune surveillance in melanoma: From immune attack to melanoma escape and even counterattack. Cancer Biol Ther. 2017;18(7):451–69. [PubMed: 28513269]
31. Taube JM, Anders RA, Young GD, et al. Colocalization of inflammatory response with B7-h1 expression in human melanocytic lesions supports an adaptive resistance mechanism of immune escape. Sci Transl Med. 2012;4(127):127ra37.
32. Orecchioni M, Ghosheh Y, Pramod AB, et al. Macrophage Polarization: Different Gene Signatures in M1(LPS+) vs. Classically and M2(LPS-) vs. Alternatively Activated Macrophages. Front Immunol. 2019;10:1084. [PubMed: 31178859]
33. Hao NB, Lu MH, Fan YH, et al. Macrophages in tumor microenvironments and the progression of tumors. Clin Dev Immunol. 2012;2012:948098.
34. Makitie T, Summanen P, Tarkkanen A, et al. Tumor-infiltrating macrophages (CD68(+) cells) and prognosis in malignant uveal melanoma. Invest Ophthalmol Vis Sci. 2001;42(7):1414–21. [PubMed: 11381040]
35. Kiss J, Timar J, Somlai B, et al. Association of microvessel density with infiltrating cells in human cutaneous malignant melanoma. Pathol Oncol Res. 2007;13(1):21–31. [PubMed: 17387385]
36. Shi L, Lei D, Ma C, et al. Clinicopathological implications of tumour-associated macrophages and vascularization in sinonasal melanoma. J Int Med Res. 2010;38(4):1276–86. [PubMed: 20926000]
37. Chen P, Huang Y, Bong R, et al. Tumor-associated macrophages promote angiogenesis and melanoma growth via adrenomedullin in a paracrine and autocrine manner. Clin Cancer Res. 2011;17(23):7230–9. [PubMed: 21994414]
38. Jensen TO, Schmidt H, Moller HJ, et al. Macrophage markers in serum and tumor have prognostic impact in American Joint Committee on Cancer stage I/II melanoma. J Clin Oncol. 2009;27(20):3330–7. [PubMed: 19528371]
39. Tsujikawa T, Kumar S, Borkar RN, et al. Quantitative Multiplex Immunohistochemistry Reveals Myeloid-Inflamed Tumor-Immune Complexity Associated with Poor Prognosis. Cell Rep. 2017;19(1):203–17. [PubMed: 28380359]
40. Erdag G, Schaefer JT, Smolkin ME, et al. Immunotype and immunohistologic characteristics of tumor-infiltrating immune cells are associated with clinical outcome in metastatic melanoma. Cancer Res. 2012;72(5):1070–80. [PubMed: 22266112]
41. Schroder K, Hertzog PJ, Ravasi T, et al. Interferon-gamma: an overview of signals, mechanisms and functions. J Leukoc Biol. 2004;75(2):163–89. [PubMed: 14525967]
42. Dengel LT, Norrod AG, Gregory BL, et al. Interferons induce CXCR3-cognate chemokine production by human metastatic melanoma. J Immunother. 2010;33(9):965–74. [PubMed: 20948440]
43. Barker JN, Karabin GD, Stoof TJ, et al. Detection of interferon-gamma mRNA in psoriatic epidermis by polymerase chain reaction. J Dermatol Sci. 1991;2(2):106–11. [PubMed: 1905950]
44. Livden JK, Nilsen R, Bjerke JR, et al. In situ localization of interferons in psoriatic lesions. Arch Dermatol Res. 1989;281(6):392–7. [PubMed: 2480752]
45. Di Nuzzo S, Sylva-Steenland RM, Koomen CW, et al. UVB irradiation of normal human skin favors the development of type-2 T-cells in vivo and in primary dermal cell cultures. Photochem Photobiol. 2002;76(3):301–9. [PubMed: 12403451]
46. Pellegrino A, Antonaci F, Russo F, et al. CXCR3-binding chemokines in multiple myeloma. Cancer Lett. 2004;207(2):221–7. [PubMed: 15072832]

47. Flier J, Boorsma DM, van Beek PJ, et al. Differential expression of CXCR3 targeting chemokines CXCL10, CXCL9, and CXCL11 in different types of skin inflammation. J Pathol. 2001;194(4):398–405. [PubMed: 11523046]

48. Pardoll DM. The blockade of immune checkpoints in cancer immunotherapy. Nat Rev Cancer. 2012;12(4):252–64. [PubMed: 22437870]

49. Tumeh PC, Harview CL, Yearley JH, et al. PD-1 blockade induces responses by inhibiting adaptive immune resistance. Nature. 2014;515(7528):568–71. [PubMed: 25428505]

50. Pollard JW. Tumour-educated macrophages promote tumour progression and metastasis. Nat Rev Cancer. 2004;4(1):71–8. [PubMed: 14708027]

51. Gordon SR, Maute RL, Dulken BW, et al. PD-1 expression by tumour-associated macrophages inhibits phagocytosis and tumour immunity. Nature. 2017;545(7655):495–9. [PubMed: 28514441]

52. Chao MP, Alizadeh AA, Tang C, et al. Anti-CD47 antibody synergizes with rituximab to promote phagocytosis and eradicate non-Hodgkin lymphoma. Cell. 2010;142(5):699–713. [PubMed: 20813259]

53. Hartley GP, Chow L, Ammons DT, et al. Programmed Cell Death Ligand 1 (PD-L1) Signaling Regulates Macrophage Proliferation and Activation. Cancer Immunol Res. 2018;6(10):1260–73. [PubMed: 30012633]

54. Xiong H, Mittman S, Rodriguez R, et al. Anti-PD-L1 Treatment Results in Functional Remodeling of the Macrophage Compartment. Cancer Res. 2019;79(7):1493–506. [PubMed: 30679180]

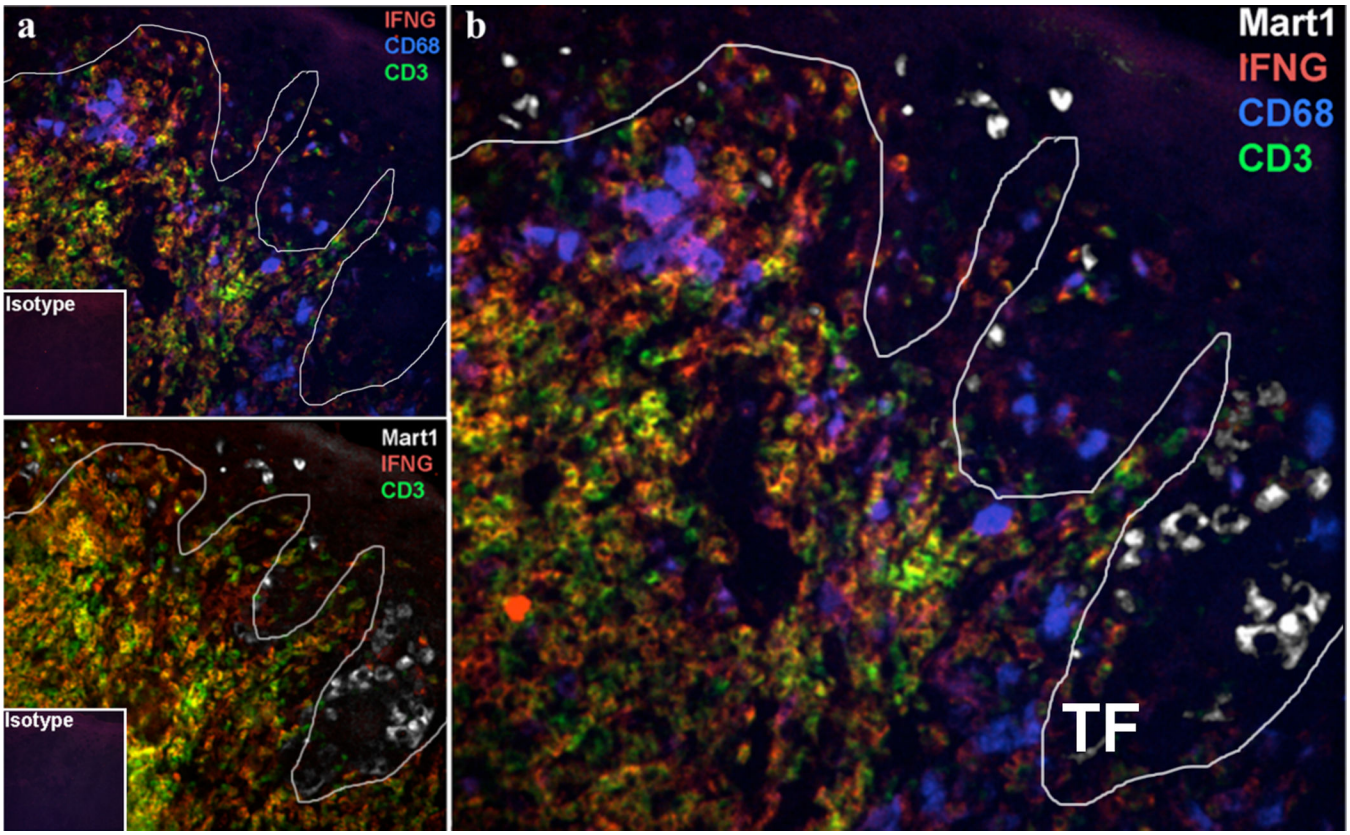

FIG. 1.

Microanatomic distribution of IFN-γ producing macrophages and lymphocytes close to the melanoma invasive front. a) Immunofluorescence of two serial frozen sections of primary melanoma tissue of IFN-γ (red), CD3 lymphocyte (green), CD68 macrophage (blue), and MART-1 melanoma (white). b) Overlay of serial sections that demonstrates proximity and distribution of immune cells relative to the melanoma tumor front (TF) indicated by the white line.

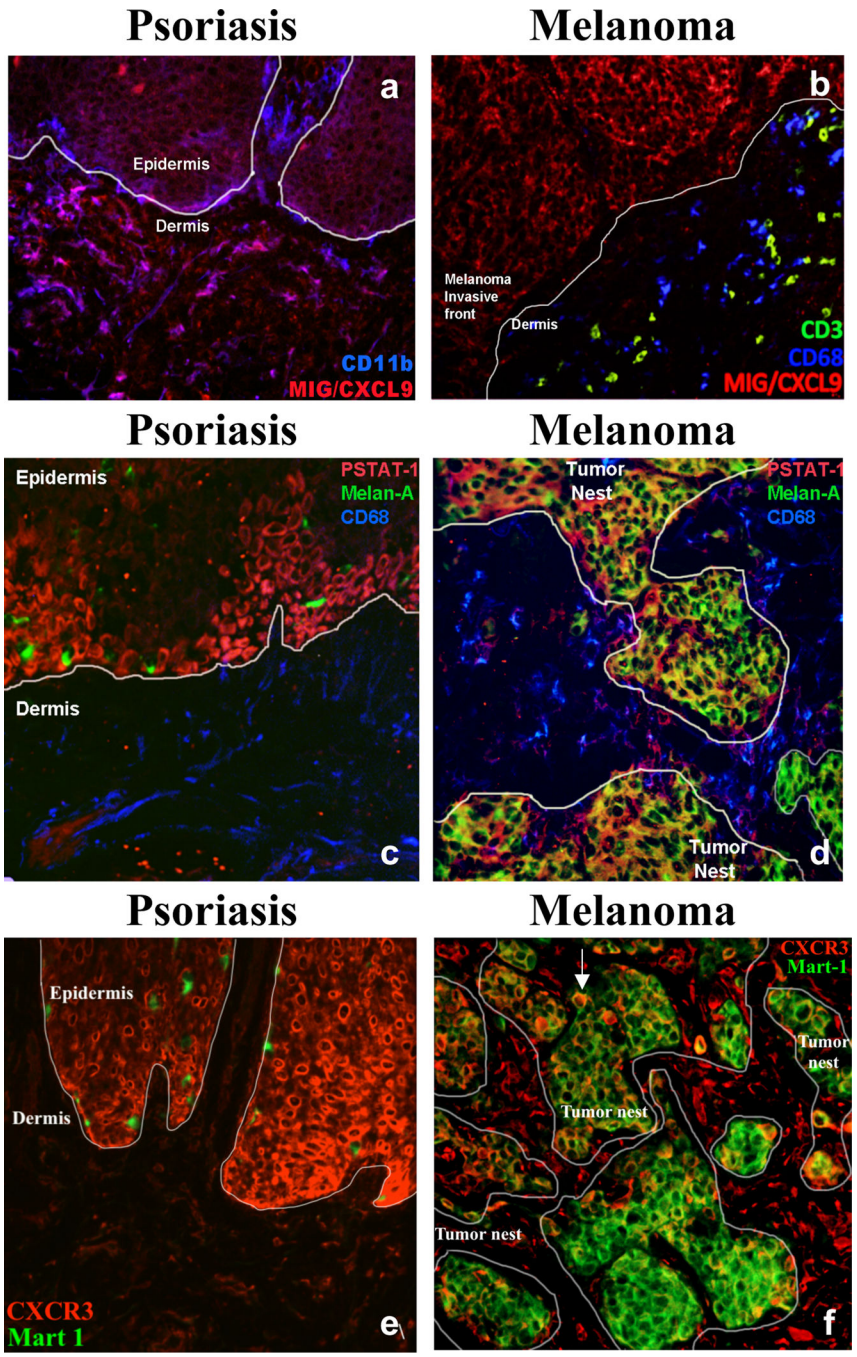

FIG. 2.

Immunofluorescence of MIG/CXCL, P-STAT-1(Y701), and CXCR3 in psoriasis and melanoma tissue. a) Co-localization of MIG/CXCL9 (red) and CD11b myeloid cells (blue) in psoriasis tissue and b) MIG/CXCL9 (red), CD68 macrophages (blue), and CD3 lymphocytes (green) in melanoma tissue c) co-localization of P-STAT-1(Y701) (red), CD68 macrophages (blue), and Melan-A positive melanocytes (green) in psoriasis tissue and d) co-localization of P-STAT-1(Y701) (red), CD68 macrophages (blue), and Melan-A positive melanoma tumor cells (green) in melanoma tissue, e) Co-localization of CXCR3 (red) and

MART-1 positive melanocytes (green) in psoriasis tissue and f) Co-localization of CXCR3 (red) and MART-1 positive melanoma tumor cells (green) in melanoma tissue. White arrow indicates melanoma tumor cells stained with both CXCR3 and MART-1.

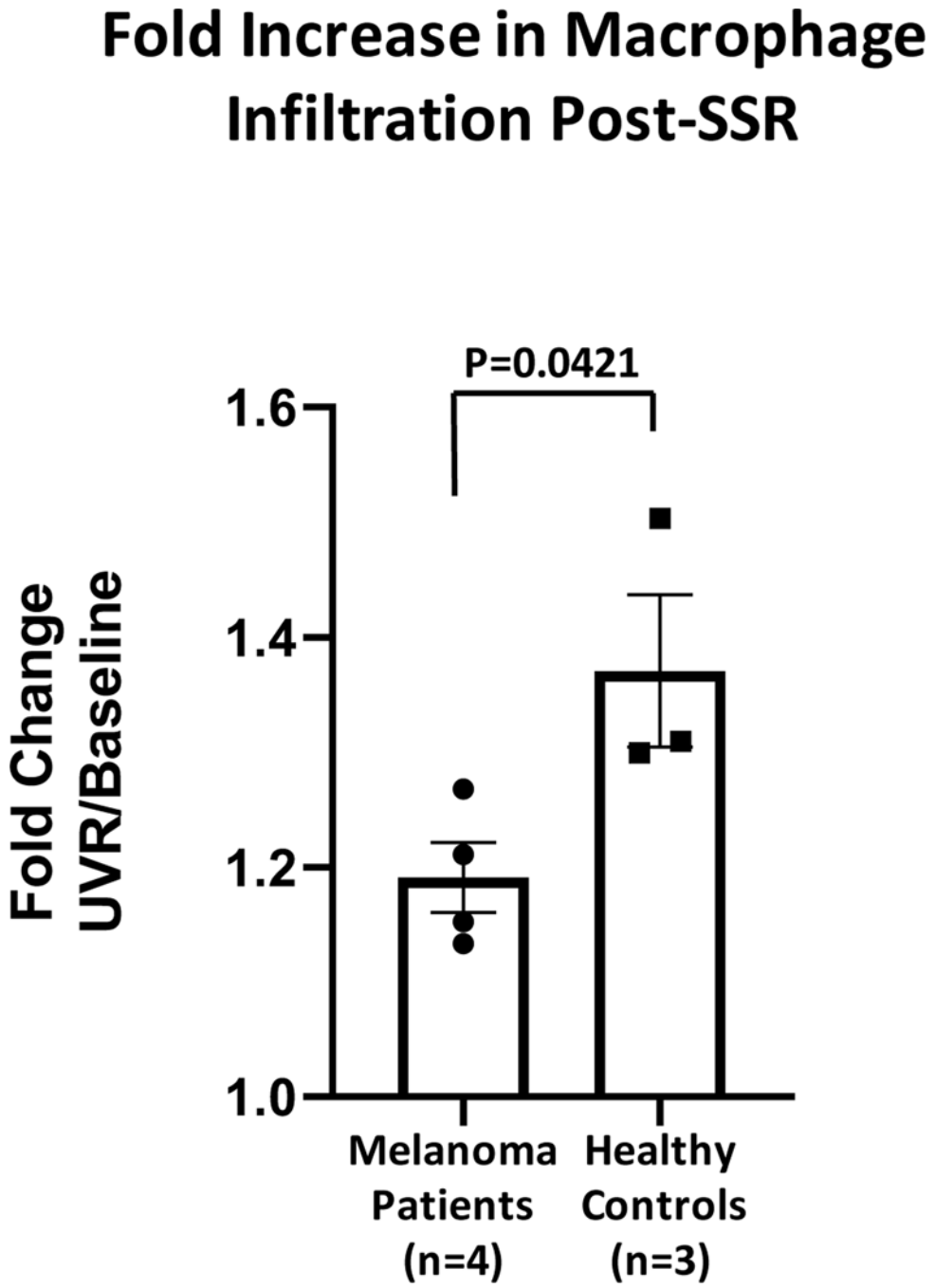

FIG. 3.

Quantitation of the increase in density of macrophage infiltration post-SSR exposure in melanoma patients (n=4) and healthy controls (n=3).

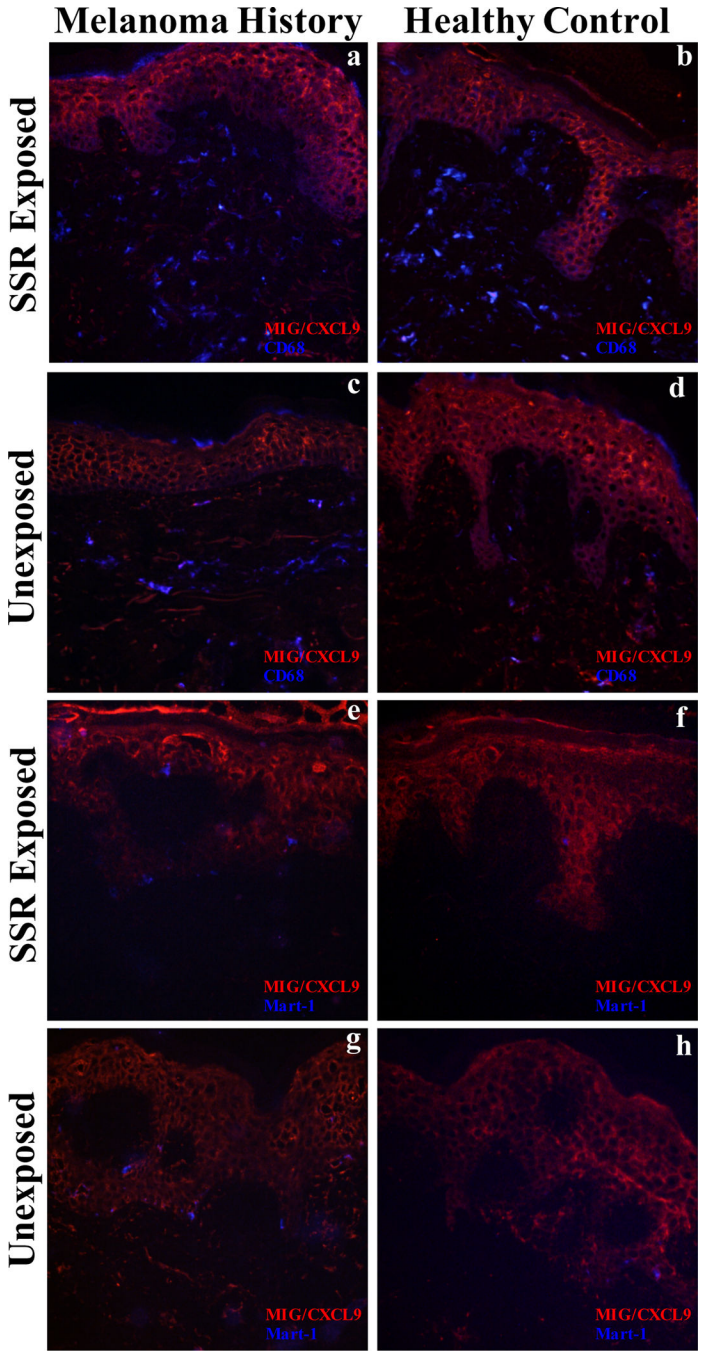

FIG. 4.

Immunofluorescence of MIG/CXCL and macrophages in simulated solar radiation (SSR) exposed skin of melanoma patients and healthy controls. Double immunofluorescence for CD68 macrophages (blue) and MIG/CXCL9 (red) in melanoma patients after (a) and before (c) SSR exposure and in a healthy control subject after (b) and before (d) SSR exposure. Double immunofluorescence for Mart-1 positive melanocytes (blue) and MIG/CXCL9 (red)

in melanoma patients after (e) and before (g) SSR exposure and in a healthy control subject after (f) and before (h) SSR exposure.

TABLE 1.

Part 1 Patient Demographics.

Age	Gender	Location	Type	Breslow's	Ulceration	Mitosis	Stage
48	M	R chest/abdomen	superficial spreading	>5 mm	Y	5	IIIB (T4b, N1a, Mx)
71	M	R chest	superficial spreading	2.33 mm	N	1	IIIB (T3b, N2a, M0)
49	F	R chest	superficial spreading	>1.53 mm	N	2	IIIA (T2a, N1a, M0)
74	M	Right back	superficial spreading	1.9 mm	N	1	IB (T2a, N0, Mx)
42	F	Mid back	superficial spreading	0.88 mm	N	1	IB (T1b, N0, Mx)
90	M	Left back	MIS superficial spreading	n/a	N	n/a	0(Tis, Nx, Mx)
41	F	L chest	MIS superficial spreading	n/a	N	n/a	0(Tis, Nx, Mx)
72	F	R cheek	MIS Lentigo Maligna	n/a	N	n/a	0(Tis, Nx, Mx)
60	M	R cheek	MIS Lentigo Maligna	n/a	N	n/a	0(Tis, Nx, Mx)
92	M	R ear lobe	MIS Lentigo Maligna	n/a	N	n/a	0(Tis, Nx, Mx)

TABLE 2.

PART 2 Enrollment Data.

#	Age	Gender	FST	MED (J/cm^2 UVB)	Melanoma Diagnosis	Type	Breslow's Depth
1	68	M	III	105	2006	Superficial Spreading	0.85
2	66	M	II	184	2009	MIS (Lentigo Maligna)	n/a
3	68	M	II	134	2000	MIS	n/a
4	65	M	II	139	1999	Superficial Spreading	1.76
5	62	M	I	124	2006	Invasive	2.8
1	45	F	II	137	Control	n/a	n/a
2	49	M	II	162	Control	n/a	n/a
3	36	F	II	120	Control	n/a	n/a
4	38	M	III	100	Control	n/a	n/a